Available online at www.sciencedirect.com
ScienceDirect
Acta Biomaterialia 4 (2008) 838–843
Acta BIOMATERIALIA
www.elsevier.com/locate/actabiomat

Layer-by-layer assembly of viral capsid for cell adhesion

Y. Lin [a,b], Z. Su [a,*], Z. Niu [c], S. Li [c], G. Kaur [c], L.A. Lee [c], Q. Wang [c,*]

[a] State Key Laboratory of Polymer Physics and Chemistry, Changchun Institute of Applied Chemistry, Chinese Academy of Sciences, Changchun, Jilin 130022, China
[b] Department of Materials Science and Engineering, Jilin University, Changchun 130025, China
[c] Department of Chemistry and Biochemistry and Nanocenter, University of South Carolina, Columbia, SC 29208, USA

Received 1 November 2007; received in revised form 21 January 2008; accepted 26 February 2008
Available online 15 March 2008

Abstract

Cowpea mosaic virus (CPMV)-based thin films are biologically active for cell culture. Using layer-by-layer assembly of CPMV and poly(diallyldimethylammonium chloride), quantitatively scalable biomolecular surfaces were constructed, which were well characterized using quartz crystal microbalance, UV–vis and atomic force microscopy. The surface coverage of CPMV nanoparticles depended on the adsorption time and pH of the virus solution, with a greater amount of CPMV adsorption occurring near its isoelectric point. It was found that the adhesion and proliferation of NIH-3T3 fibroblasts can be controlled by the coverage of viral particles using this multilayer technique.

Keywords: Cowpea mosaic virus; Layer-by-layer; Self-assembly; Cell adhesion

1. Introduction

Self-assembly of protein cages into higher-order structures offers great opportunities for developing new materials and other applications, including functional membranes, electronics, sensing and energy harvesting [1–9]. Some recent studies have shown that the layer-by-layer (LbL) assembly technique can be readily employed to construct ultrathin films of viruses and other biological particles via electrostatic interactions [9–14]. By controlling the ionic strength and pH of the solution, the LbL assembly technique enables the creation of highly tunable functional surfaces [15,16]. In particular, the LbL assembly process is highly biocompatible and generally does not interfere with the properties and natural architectures of viruses and other biomolecules [9,11,13,14].

Cowpea mosaic virus (CPMV), a plant virus ~30 nm in diameter, has had its physical, biological and genetic properties well characterized over the past few years [17–20]. The virus comprises 60 copies of two protein subunits in an icosahedral symmetry. The particles are remarkably stable, demonstrated by their application in organic reactions and as a model system in bioconjugation chemistry [20,21]. Recent studies have shown the strong interactions between CPMV with some mammalian cells [22,23]. Because the chemical structure of CPMV is well understood and can be readily modified, it is an excellent multivalent platform for tailoring the surface composition and properties to suit particular needs in surface engineering. In particular, it offers an ideal scaffold for investigating how the nanoscale surface morphology and polyvalent ligand display will affect cell response.

Here, the use of CPMV particles as a novel support for cell adhesion and proliferation is explored. By varying the coating density and surface coverage of the viral particles, it is possible to alter cell attachment and outgrowth behavior. In particular, the LbL assembly process used to control the coating density and smoothness of the surface coated with CPMV on quartz probes is thoroughly characterized.

* Corresponding authors. Tel.: +1 803 777 8436; fax: +1 803 777 9521.
E-mail addresses: zhsu@ciac.jl.cn (Z. Su), wang@mail.chem.sc.edu (Q. Wang).

1742-7061/$ - see front matter © 2008 Acta Materialia Inc. Published by Elsevier Ltd. All rights reserved.
doi:10.1016/j.actbio.2008.02.026

2. Materials and methods

2.1. Materials

Poly(diallyldimethylammonium chloride) (PDDA) aqueous solution with molecular weight ~100,000–200,000 and poly(styrenesulfonic acid) (PSS) ($M_W = 70{,}000$) were purchased from Sigma–Aldrich Co. All the chemicals were used as received without further purification. Water was purified using a Millipore Milli-Q system (18.2 MΩ).

2.2. Purification of CPMV

CPMV was obtained from cowpea plants. Cowpea plants ~2 weeks old were inoculated with CPMV. The leaves were harvested, and the virus was isolated from the host plant. The leaves were crushed and added to 0.1 M potassium-phosphate buffer at pH 7.8 with 0.2% β-mercaptoethanol. The mixture was centrifuged at 9000 rpm for 15 min before the supernatant was treated with a 1:1 ratio of $CHCl_3$:1-butanol. The aqueous portion was separated, and CPMV was precipitated by the addition of polyethylene glycol 8 K and NaCl. The resultant pellets were re-suspended in 0.1 M potassium-phosphate buffer at pH 7.8. After a final ultracentrifugation at 42,000 rpm for 2.5 h, pure CPMV obtained was re-suspended overnight in 0.1 M potassium-phosphate buffer at pH 7.8.

2.3. Quartz crystal microbalance

AT-cut quartz crystals were manufactured by Beijing Ziweixing Microelectronic Co., Ltd. The frequency was monitored by a Protek Frequency Counter (Model C3100). A crystal 9 mm in diameter was coated on both sides with silver 4.5 mm in diameter, and the resonance frequency was 9 MHz. Before each quartz crystal microbalance (QCM) experiment, the resonator was washed in ethanol solution for 10 min (followed by rinsing with pure water and drying with a stream of N_2). It was then immersed in a PDDA aqueous solution (1 mg ml^{-1}) for 20 min, taken out, washed thoroughly with pure water, and dried with a stream of N_2. The positively charged surface was further immersed in a PSS aqueous solution (2 mg ml^{-1}). This alternate cycle was repeated three times for a precursor film to provide a uniform charge and a smooth surface for subsequent deposition. The electrode with a $(PDDA/PSS)_2$/PDDA precursor film was then alternately immersed in CPMV solution for 20 min and in PDDA solution for 20 min with intermediate water washing and drying. The frequency of QCM was monitored in each adsorption step after drying.

2.4. Other measurements

Tapping-mode atomic force microscopy (AFM) images were obtained in ambient conditions using an SPA300 instrument (Seiko). Si tips with a resonance frequency of ~300 kHz, a spring constant of about 2 N m^{-1} and a scan rate of 0.5 Hz were used. UV–vis spectra of the thin films deposited on quartz slides were collected on a Shimadzu UV-2450 spectrophotometer.

3. Results and discussion

The isoelectric point (p*I*) of CPMV is about 5.5 [24], therefore at neutral pH the viruses can be considered an anionic macromolecule. In the present study, it was found that one interlayer of the cationic polyelectrolyte PDDA was able to induce binding of CPMV to the surface, which is similar to the previous report on the LbL assembly of cowpea chlorotic mottle virus [12]. In a typical experiment, the quartz crystal wafer was cleaned with H_2SO_4:H_2O_2 (7:3) solution, followed by ultrasonication three times in pure water and drying with a stream of N_2. In order to obtain a uniformly charged layer, the quartz wafer was immersed in a PDDA aqueous solution (1.0 mg ml^{-1}) for 20 min, then washed thoroughly with pure water and dried. The positively charged surface was further immersed in a PSS aqueous solution (2.0 mg ml^{-1}). This coating cycle was repeated twice, and a PDDA layer was coated as the outermost surface to denote the precursor film as $(PDDA/PSS)_2$/PDDA, where the numeric value two indicates the number of polymer bilayers. The wafer, as the QCM resonator, was alternatively immersed in CPMV solution (0.1 mg ml^{-1}) for 20 min and PDDA solution (1.0 mg ml^{-1}) for 20 min with steps of washing and drying.

The time-dependent CPMV adsorption on $(PDDA/PSS)_2$/PDDA coated quartz crystal wafer at neutral pH was monitored by QCM. In the QCM experiment, the crystal electrode was coated with Ag on both sides, so the frequency shift came from both sides. As shown in Fig. 1a, the frequency reaches a plateau when the adsorption time is 10 min, which corresponds to 113 ng of CPMV on each side of the QCM electrode calculated by Sauerbrey's equation [25]. The mass increase corresponds to a 76% coverage of the surface of the QCM electrode, assuming monolayer adsorption with spherical packing.

QCM data for CPMV and PDDA depositions are presented in Fig. 1. For each newly adsorbed CPMV layer on the quartz crystal, the average frequency shift is 229 ± 22 Hz, suggestive of a homogeneous CPMV layer. For each adsorbed PDDA layer, the average frequency shift is 35 ± 5 Hz. UV–vis absorbance was also measured to monitor the assembly process. Because PDDA in solution has only slight absorbance in the UV region [26], the UV absorption at a 240–400 nm wavelength of the composite films is primarily attributed to CPMV. Fig. 1c and d show that the absorbance at 260 nm increases linearly with the number of CPMV deposition cycles. Both QCM and UV–vis data indicate the successive deposition of PDDA/CPMV layers.

To document the influence of pH on the LbL process, CPMV solutions at four different pH levels were used to study the pH-dependent deposition behavior. First, the

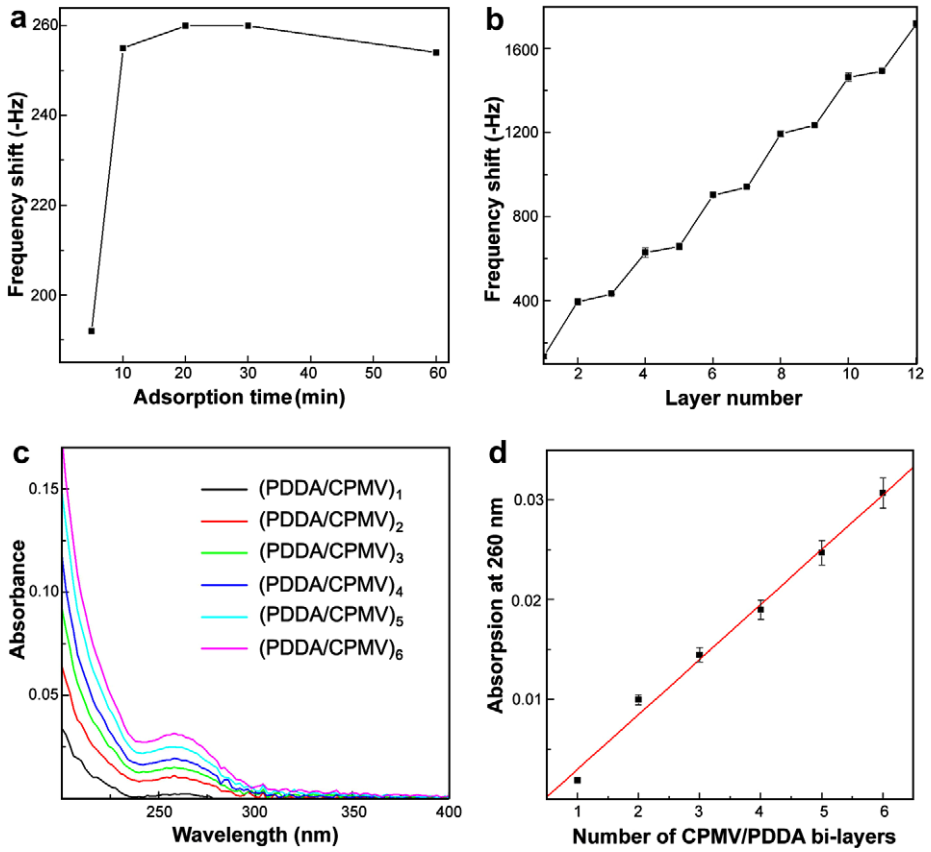

Fig. 1. (a) Time-dependent CPMV (0.1 mg ml^{-1}, pH 7.0) adsorption onto a $(PDDA/PSS)_2$/PDDA surface monitored by QCM. (b) LbL deposition of CPMV (0.1 mg ml^{-1}, pH 7.0) and PDDA (1.0 mg ml^{-1}, pH 5.6) monitored by QCM. (c) UV–vis spectra of PDDA/CPMV thin films composed of different numbers of bilayers. (d) Step growth of the absorbance at 260 nm as a function of number of bilayers deposited.

adsorption of the primary layer of CPMV was compared at various pH levels. Fig. 2a shows that, at pH 4.0, the frequency shift is 141 ± 50 Hz, which corresponds to 61 ± 22 ng of CPMV nanoparticles adsorbed onto one side of the QCM electrode, and a $41 \pm 15\%$ surface coverage of the electrode, assuming a monolayer adsorption with sphere-packing [25]. At other pH levels, the coverage of the primary CPMV layer is $88 \pm 10\%$ (pH 5.2), $76 \pm 4\%$ (pH 7.0) and $30 \pm 2\%$ (pH 9.0), respectively.

Based on these results, one can assume that both the electrostatic interactions among particles and the net charge on the protein surfaces influence the amount of CPMV deposited on the QCM electrode. The linear growth patterns for the subsequent CPMV and PDDA layers (Fig. 2a) indicate that the CPMV and PDDA depositions are uniform in each cycle. Fig. 2b shows the average frequency shift for each CPMV layer, which corresponds to the average CPMV coverage of $14 \pm 2\%$ (pH 4.0),

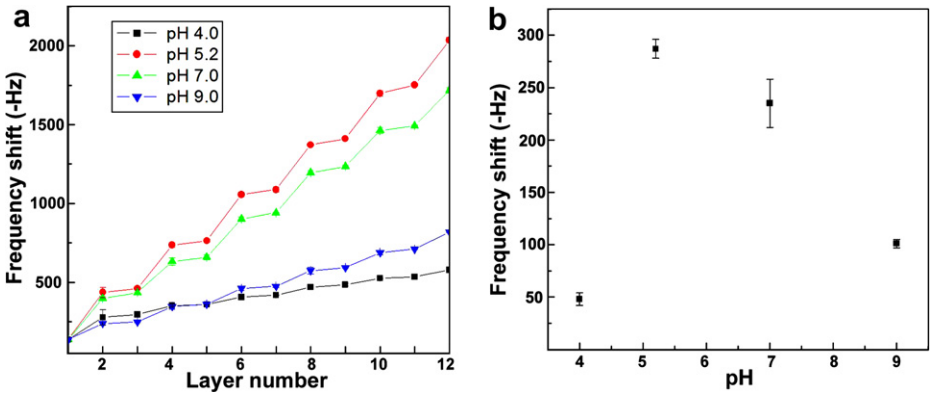

Fig. 2. (a) Frequency shifts of the QCM against the PDDA/CPMV deposition at different pH of the CPMV solution (0.1 mg ml^{-1}). The PDDA concentration was 1.0 mg ml^{-1} (pH 5.6). (b) Average QCM frequency shifts associated with one CPMV layer at different pH (of the CPMV solution).

83 ± 2% (pH 5.2), 67 ± 6% (pH 7.0), and 29 ± 1% (pH 9.0).

Although the overall net charge of CPMV is positive at pH 4.0 (below its isoelectric point), depositing small amounts of CPMV on positive charged surface is still possible owing to some negatively charged groups on its outer surface [24]. However, this condition is sub-optimal owing to the repulsion between the particles and surfaces. At pH 5.2 (near its p*I*), the net neutral charge on CPMV results in the attraction of particles to lower the surface energy. At this point, maximum adsorption was achieved, which was consistent with reported studies for LbL deposition of proteins and other biological particles [9,27]. At pH 7.0 and pH 9.0, the net charge of CPMV is negative, and the particles are expected to adsorb strongly onto the positively charged surfaces. However, the strong repulsion among the particles would prohibit a higher percentage of surface coverage, as indicated by the results, i.e., the surface coverage at pH 9.0 was merely 30 ± 2%.

Images obtained from AFM also support these results obtained from QCM. When the pH of the PDDA solution is fixed at 5.6 for the first CPMV layer coated (pH 4.0), the quartz surface is only partially covered with viral particles (Fig. 3a). At pH 5.2, near the p*I* of CPMV, even with one layer of coating, the entire surface is better covered with CPMV (Fig. 3b) than in any other pH conditions. As shown in Fig. 3c and d, after six layers of CPMV adsorbed on the quartz wafer, the surface was completely covered with CPMV. Moreover, a smoother surface (RMS 5.2 nm) is obtained at pH 5.2 after six layers of CPMV adsorption, while the surface was more rough (RMS 9.4 nm) at pH 4.0 after six layers of CPMV adsorption.

It is well known that the interactions between the cell and the material are influenced by many factors such as surface wettability, chemistry, roughness and the existence of bioactive factors [27–29]. The authors have been particularly interested in manipulating such physical attributes of the plant viruses for various applications, including potential use as bioscaffolds for probing cell behaviors. Furthermore, the LbL assembly method offers a practical way of controlling the surface coverage of viral particles, which therefore would affect the cell response. NIH-3T3 fibroblasts were selected for the preliminary study. PDDA was used as the polyelectrolyte, owing to its cell-repellent property [30].

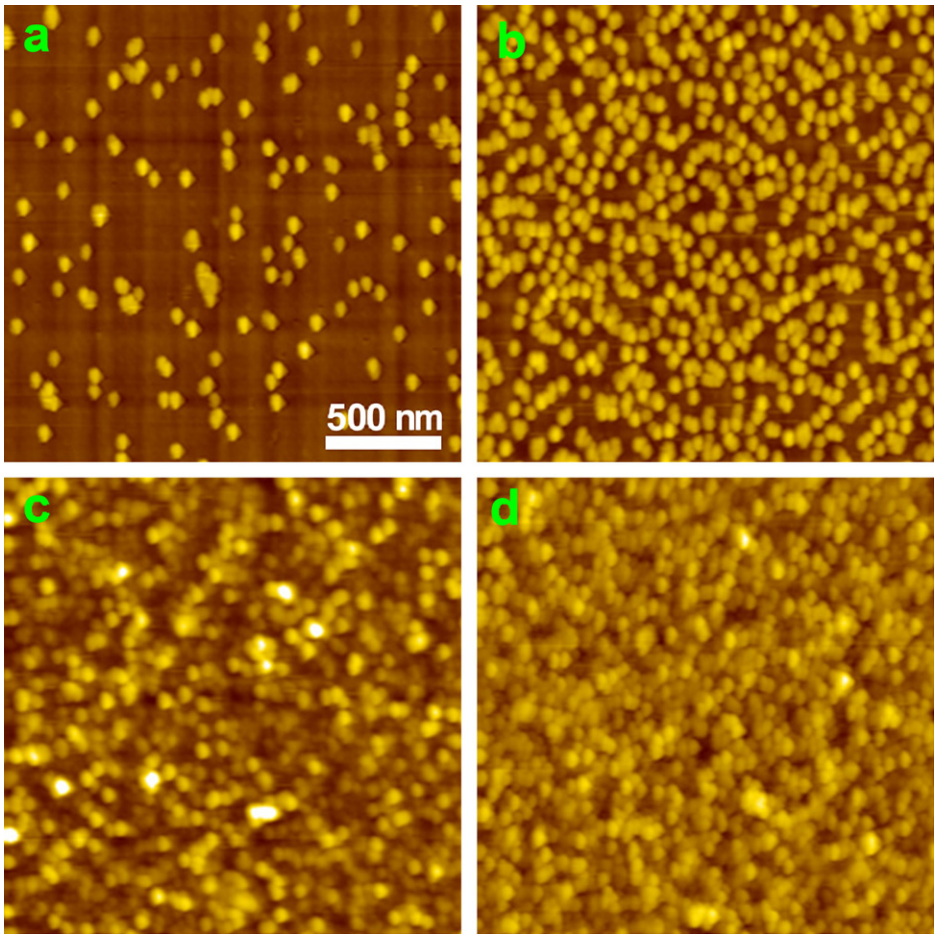

Fig. 3. AFM height images of PDDA/CPMV thin films at different pH of the CPMV solution (0.1 mg ml^{-1}): (a) $(PDDA/CPMV)_1$, pH 4.0; (b) $(PDDA/CPMV)_1$, pH 5.2; (c) $(PDDA/CPMV)_6$, pH 4.0; and (d) $(PDDA/CPMV)_6$, pH 5.2. All the images have the same scale bar.

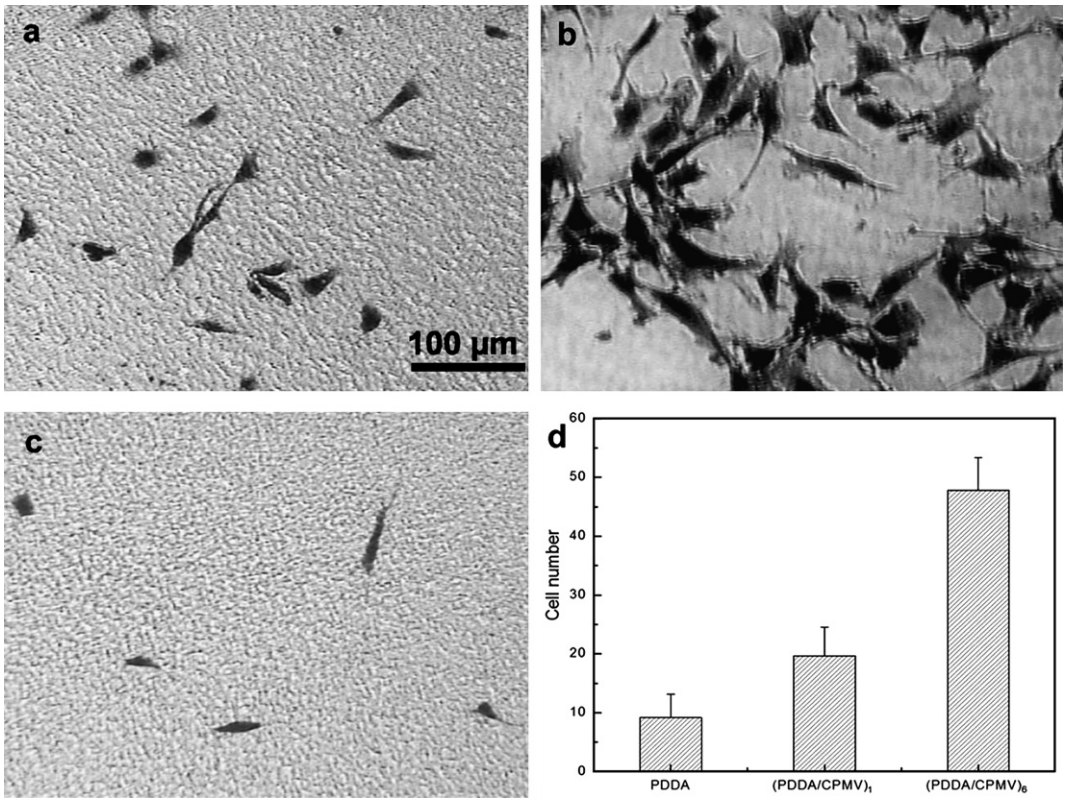

Fig. 4. Optical images of NIH-3T3 fibroblast cells attached on: (a) $(PDDA/CPMV)_1$, pH 4.0; (b) $(PDDA/CPMV)_6$, pH 4.0; (c) $(PDDA/PSS)_5$ PDDA (negative control); and (d) numbers of cell attached on different substrates.

For cell studies, PDDA/CPMV coated quartz wafers were placed in 12-well tissue culture plate, and each well was seeded with 1.3×10^4 cells ml^{-1} in DMEM complete growth media (high glucose DMEM supplemented with 10% bovine calf serum, 4 mM L-glutamine, 1 × penicillin and streptomycin). After 24 h, the wells were washed three times in 1 × PBS (pH 7.4), and the attached cells were fixed with 3% glutaraldehyde at room temperature for 10 min. The samples were rinsed in PBS buffer, and the cells were stained with 1% Giemsa stain for 30 min. Cell attachment and cell morphology were observed under an inverted, phase-contrast microscope (Fig. 4a–c). For each condition, three parallel experiments were performed, and the cell numbers with standard deviation are reported in Fig. 4d. With $(PDDA/PSS)_5$/PDDA as negative control, where the PDDA was the outermost layer, few cells were observed (Fig. 4c). In comparison, with $(PDDA/CPMV)_1$ and $(PDDA/CPMV)_6$ as substrates, CPMV being the outermost layer, efficient cell adhesion was observed (Fig. 4a and b). In comparing cell adhesion on $(PDDA/CPMV)_1$ and $(PDDA/CPMV)_6$, it was noticed that the surface coverage of CPMV is a very important factor for cell attachment and spreading. In addition, as the $(PDDA/CPMV)_6$ surface has much better virus coverage than the $(PDDA/CPMV)_1$ coated surface (Fig. 3a and c), the former surface evidently showed much more cell attachment. Moreover, the cells exhibited similar spreading and spindle formations to cells cultured on polystyrene (conventional cell culture coatings). This demonstrates the feasibility of using CPMV to induce cell adhesion and cultivation with no observable cytotoxicity towards the mammalian cells. In addition, the plant virus particles offer the added features of high processibility via chemical conjugations and genetic modifications to modulate the cell behavior further.

In summary, PDDA/CPMV LbL assemblies in aqueous solutions were investigated and characterized using QCM, UV–vis, and AFM. Ultrathin films were successively prepared by alternatively adsorbing CPMV and PDDA. The surface coverage of CPMV nanoparticles depended on adsorption time and pH of the virus solution, with the greatest amount of CPMV adsorption occurring near its p*I*. It was demonstrated that virus-based thin films are biologically active for cell culture and that the coverage of viral particles is enhanced by this multilayer LbL technique, which effectively improves cell adhesion and survival. The results from this study show that a well-defined plant virus surface provides a very promising scaffold for the study of cell adhesion and can be expanded to the investigation of other cell response behavior.

Acknowledgements

This work was partially supported by NSF-CAREER Award, US Army-MURI program, DOD-DURIP and the W.M. Keck Foundation. Financial support from the National Natural Science Foundation of China (Nos.

50403008, 20423003 and 50621302) is gratefully acknowledged. NIH-3T3 fibroblast cells were kindly obtained from Professor W. Stephen Kistler.

References

[1] Douglas T, Young M. Viruses: making friends with old foes. Science 2006;312:873–5.
[2] Flynn CE, Lee SW, Peelle BR, Belcher AM. Viruses as vehicles for growth, organization and assembly of materials. Acta Mater 2003;51:5867–80.
[3] Matsui T, Matsukawa N, Iwahori K, Sano KI, Shiba K, Yamashita I. Realizing a two-dimensional ordered array of ferritin molecules directly on a solid surface utilizing carbonaceous material affinity peptides. Langmuir 2007;23:1615–8.
[4] Lin Y, Boker A, He J, Sill K, Xiang H, Abetz C, et al. Self-directed self-assembly of nanoparticle/copolymer mixtures. Nature 2005;434:55–9.
[5] Russell JT, Lin Y, Boker A, Long S, Carl P, Zettl H, et al. Self-assembly and cross-linking of bionanoparticles at liquid–liquid interfaces. Angew Chem Int Ed 2005;44:2420–6.
[6] Niu Z, Bruckman MA, Kotakadi VS, He J, Emrick T, Russell TP, et al. Study and characterization of tobacco mosaic virus head-to-tail assembly assisted by aniline polymerization. Chem Commun 2006:3019–21.
[7] Strable E, Johnson JE, Finn MG. Natural nanochemical building blocks: icosahedral virus particles organized by attached oligonucleotides. Nano Lett 2004;4:1385–9.
[8] Cheung CL, Chung SW, Chatterji A, Lin TW, Johnson JE, Hok S, et al. Physical controls on directed virus assembly at nanoscale chemical templates. J Am Chem Soc 2006;128:10801–7.
[9] Yoo PJ, Nam KT, Qi J, Lee SK, Park J, Belcher AM, et al. Spontaneous assembly of viruses on multilayered polymer surfaces. Nature Mater 2006;5:234–40.
[10] Fischlechner M, Reibetanz U, Zaulig M, Enderlein D, Romanova J, Leporatti S, et al. Fusion of enveloped virus nanoparticles with polyelectrolyte-supported lipid membranes for the design of bio/nonbio interfaces. Nano Lett 2007;7:3540–6.
[11] Nam KT, Kim DW, Yoo PJ, Chiang CY, Meethong N, Hammond PT, et al. Virus-enabled synthesis and assembly of nanowires for lithium ion battery electrodes. Science 2006;312:885–8.
[12] Suci PA, Klem MT, Arce FT, Douglas T, Young M. Assembly of multilayer films incorporating a viral protein cage architecture. Langmuir 2006;22:8891–6.
[13] Lvov Y, Hass H, Decher G, Mohwald H. Successive deposition of alternate layers of polyelectrolytes and a charged virus. Langmuir 1994;10:4232–6.
[14] Lvov Y, Ariga K, Ichinose I, Kunitake T. Assembly of multicomponent protein films by means of electrostatic layer-by-layer adsorption. J Am Chem Soc 1995;117:6117–23.
[15] Zhang X, Chen H, Zhang H. Layer-by-layer assembly: from conventional to unconventional methods. Chem Commun 2007:1395.
[16] Decher G. Fuzzy nanoassemblies: toward layered polymeric multicomposites. Science 1997;277:1232–7.
[17] Lee LA, Wang Q. Adaptations of nanoscale viruses and other protein cages for medical applications. Nanomedicine 2006;2:137–49.
[18] Wang Q, Kaltgrad E, Lin T, Johnson JE, Finn MG. Natural supramolecular building blocks: wild-type cowpea mosaic virus. Chem Biol 2002;9:805–11.
[19] Wang Q, Lin T, Johnson JE, Finn MG. Natural supramolecular building blocks: cysteine-added mutants of cowpea mosaic virus. Chem Biol 2002;9:813–9.
[20] Wang Q, Chan T, Hilgraf R, Finn MG, Valery VF, Sharpless KB. Ligation to protein by copper(I)-catalyzed azide-alkyne cycloaddition. J Am Chem Soc 2003;125:3192–3.
[21] Wang Q, Lin T, Tang L, Johnson JE, Finn MG. Icosahedral virus particles as addressable nanoscale building blocks. Angew Chem Int Ed 2002;41:459–62.
[22] Rae CS, Wei KI, Wang Q, Destito G, Gonzalez MJ, Singh P, et al. Systemic trafficking of plant virus nanoparticles in mice via the oral route. Virology 2005;343:224–35.
[23] Koudelka KJ, Rae CS, Gonzalez MJ, Manchester M. Interaction between a 54-kD mammalian cell surface protein and cowpea mosaic virus. J Virol 2007;81:1632–40.
[24] Chatterji A, Ochoa WF, Takafumi Ueno, Lin T, Johnson JE. A virus-based nanoblock with tunable electrostatic properties. Nano Lett 2005;5:597–602.
[25] Sauerbrey G. The use of quartz oscillators for weighing thin layers and for microweighing. Z Phys 1959;155:206–22.
[26] Shutava T, Prouty M, Kommireddy D, Lvov Y. pH responsive decomposable layer-by-layer nanofilms and capsules on the basis of tannic acid. Macromolecules 2005;38:2850–8.
[27] Khorasani MT, MoemenBellah S, Mirzadeh H, Sadatnia B. Effect of surface charge and hydrophobicity of polyurethanes and silicone rubbers on L929 cells response. Colloid Surf B: Biointerf 2006;51:112–9.
[28] Zhu Y, Gao C, He T, Liu X, Shen J. Layer-by-layer assembly to modify poly(L-lactic acid) surface toward improving its cytocompatibility to human endothelial cells. Biomacromolecules 2003;4:446–52.
[29] Ruoslahti E. Stretching is good for a cell. Science 1997;276:1345–6.
[30] Mohammed JS, DeCoster MA, McShane MJ. Micropatterning of nanoengineered surfaces to study neuronal cell attachment in vitro. Biomacromolecules 2004;5:1745–55.